Safety-Critical Finite-Time Cooperative Control for Sampled Multi-Robot Systems

Liang Gao, Yongfeng Gao, Mingde He, Changyi Xu, and Yuhu Wu

***Abstract*—We present a safety-critical finite-time control framework for sampled-data multi-robot system coordination. We formally define and construct a finite-time discrete control Lyapunov function (FT-DCLF) and derive sufficient conditions that ensure convergence within a preset number of sampling steps, thereby enhancing both applicability and convergence speed. In parallel, we improve upon a discrete control barrier function (DCBF) constraint. This constraint addresses the continuous-discrete mismatch ("safety gap") and ensures all-time safety, while mitigating deadlock and resolving performance-safety conflicts that are common in conventional DCBFs for obstacle avoidance. Both components, along with input bounds, are integrated into a single quadratically constrained quadratic program (QCQP), augmented with feasibility-aiding slack variables for real-time implementation. Simulation results demonstrate that the proposed method outperforms conventional DCLF-DCBF approaches.**

***Index Terms*—Safety-critical control, discrete control barrier function (DCBF), finite-time discrete control Lyapunov function (FT-DCLF), cooperative control**

I. Introduction

Multi-robot cooperative control has significant application value in scenarios such as unmanned inspection, warehouse logistics, and emergency search and rescue [1–3]. However, most robots exhibit nonlinear and nonholonomic characteristics [4, 5], which pose substantial challenges for multi-robot control. As group density increases and task constraints become more complex, a central challenge arises: achieving rapid convergence while ensuring collision-free navigation, under nonholonomic constraints and input constraints. In particular, within the sampled-data control framework, directly discretizing continuous-time designs often introduces "safety gaps" and feasibility issues, thereby intensifying the trade-off between safety and performance [6].

Existing research on cooperative control has mainly followed three technical directions. First, consensus and graph-theoretic approaches establish criteria for consensus conditions and convergence rates under a given communication topology [7, 8]. Second, virtual structure and leader-follower paradigms provide a systematic framework for coordinating cooperative robots based on position, displacement, or distance constraints [9, 10]. Third, the model predictive control (MPC) framework achieves coordinated performance-stability design by explicitly embedding nonlinear constraints [11]. The aforementioned approaches [7–11] typically guarantee asymptotic or exponential convergence but lack finite-time or fixed-time bounds on "when to arrive". To enhance convergence rate, finite-time and fixed-time controls have attracted increasing attention in recent years. In Ref. [12], a signal-generator-based finite-time control scheme was proposed to achieve formation control of heterogeneous multi-agent systems subject to disturbances. Subsequently, Ref. [13] developed a distributed finite-time tracking control method that ensures practical finite-time stability of quadrotor formations while avoiding Zeno behavior. In addition, Ref. [14] presented a fixed-time prescribed performance control strategy to realize leader-follower trajectory tracking of multiple wheeled mobile robots (WMRs). However, these results are mostly established without explicit state safety constraints, and thus obstacle avoidance during the convergence process is not guaranteed.

Traditional artificial potential field methods have been widely adopted for robotic obstacle avoidance due to their simplicity and online efficiency [15, 16]. However, these methods are prone to local minima and sensitive to parameter tuning, thus lacking global guarantees. Geometric velocity-domain approaches, such as velocity obstacles [17], enable real-time performance and distributed implementation, yet they often rely on assumptions about feasible relative velocities and acceleration capabilities. Consequently, these methods may become conservative or even infeasible under nonholonomic constraints and input saturation. To obtain formal safety guarantees, continuous-time control barrier functions (CBFs) and control Lyapunov functions (CLFs), together with the quadratic-program-based CLF-CBF synthesis framework (CLF-CBF-QP), provide systematic tools for establishing forward invariance and optimization-based synthesis [18, 19]. Nevertheless, most of these designs are formulated in continuous time; when directly implemented under sample-and-hold control, a "safety gap" can lead to increased conservatism or infeasibility.

To address these challenges from a safety-performance co-

Manuscript received: 19 September 2025; revised: 27 October 2025; accepted: 7 November 2025. *(Corresponding author: Yuhu Wu.)*

Citation: L. Gao, Y. Gao, M. He, C. Xu, and Y. Wu, Safety-critical finite-time cooperative control for sampled multi-robot systems, *Int. J. Intell. Control Syst.*, 2025, 30(4), 321–327.

Liang Gao, Yongfeng Gao, Mingde He, Changyi Xu, and Yuhu Wu are with School of Control Science and Engineering, Key Laboratory of Intelligent Control and Optimization for Industrial Equipment of Ministry of Education, Dalian 116024, China, and also with School of Control Science and Engineering, Dalian University of Technology, Dalian 116024, China (e-mail: gliang@mail.dlut.edu.cn; gaoyongfeng@dlut.edu.cn; hemingde@mail.dlut.edu.cn; ChangyiXU@dlut.edu.cn; wuyuhu@dlut.edu.cn).

Digital Object Identifier 10.62678/IJICS202512.10240

design perspective tailored to sampled-data systems, this paper presents a safety-critical finite-time controller. The proposed controller integrates a discrete control barrier function (DCBF) with a finite-time discrete control Lyapunov function (FT-DCLF) within a unified framework. The key idea is to impose a discrete, incremental barrier constraint at sampling instants to encode forward invariance and eliminate inter-sample safety violations, while the FT-DCLF enforces a tunable finite-time convergence rate for the closed-loop system. Both components, along with input bounds, are jointly solved within a single quadratically constrained quadratic program (QCQP) to design a controller that satisfies stringent safety and performance requirements. The main contributions of this paper are summarized as follows:

(1) We formally define the FT-DCLF and derive sufficient conditions guaranteeing convergence within a preset number of sampling steps; furthermore, we construct an FT-DCLF for WMRs to enhance applicability in complex scenarios and accelerate convergence.

(2) We improve a DCLF-based safety constraint and apply it to the cooperative control of sampled multi-WMR systems, bridging the "safety gap" of conventional DCBFs and ensuring that WMRs remain safe throughout the entire process.

(3) We integrate the DCBF, FT-DCLF, and input constraints into a single QCQP, augmented with feasibility-enhancing slack variables and tunable weights, to synthesize an enhanced safety-critical cooperative controller.

Throughout this paper, $\mathbb{R}$ denotes the set of real numbers, $\mathbb{R}^n$ denotes the set of $n\times 1$ real column vectors, $\mathbb{R}^{n\times m}$ denotes the set of $n\times m$ real matrices, $\mathbb{Z}$ denotes the set of integers, and $\mathbb{Z}_{\geqslant 0}$ denotes the set of positive integers. We use $\|\cdot\|$ for the Euclidean vector norm in $\mathbb{R}^n$. Finally, the $\lceil \kappa \rceil$ is ceiling function denoting the smallest integer greater than or equal to κ.

II. Preliminaries and Problem Formulation

A. Preliminaries

Consider a continuous-time control-affine system modeled as

$$\dot{\boldsymbol{x}} = \boldsymbol{f}(\boldsymbol{x}) + \boldsymbol{g}(\boldsymbol{x})\boldsymbol{u} \tag{1}$$

where $\boldsymbol{x}\in\mathbb{R}^n$ is the state vector, $\boldsymbol{u}\in\mathcal{U}\subset\mathbb{R}^m$ denotes the control input constrained to a compact set $\mathcal{U}$, and the vector fields $\boldsymbol{f}:\mathbb{R}^n\to\mathbb{R}^n$ and $\boldsymbol{g}:\mathbb{R}^n\to\mathbb{R}^{n\times m}$ are assumed to be locally Lipschitz continuous.

In many practical applications, the system state evolves continuously, while the control input is updated only at discrete sampling instants $t_k = kT$, where $T>0$ is the fixed sampling period. A zero-order hold (ZOH) mechanism is employed to maintain the input constant over each interval $[t_k, t_{k+1})$. It is commonly assumed that the state is measured exclusively at these sampling instants; hence, the control input $\boldsymbol{u}$, the system dynamics $\boldsymbol{f}$, and the input gain matrix $\boldsymbol{g}$ are updated solely at these times. Within each sampling interval, the following holds

$$\boldsymbol{u}(t) = \boldsymbol{u}_k,\ \forall t\in[t_k, t_{k+1}),$$

while the state $\boldsymbol{x}(t)$ evolves continuously according to the system dynamics under this piecewise-constant input. Here, $\boldsymbol{x}_k := \boldsymbol{x}(t_k)$ and $\boldsymbol{x}_{k+1} := \boldsymbol{x}(t_{k+1})$ represent the system states at two consecutive sampling instants.

To characterize safety, we define a continuously differentiable scalar function $B:\mathbb{R}^n\to\mathbb{R}$ and specify the safe set as

$$\mathcal{D} := \{\boldsymbol{x}\in\mathbb{R}^n \mid B(\boldsymbol{x})\geqslant 0\} \tag{2}$$

We assume that $B(\cdot)$ is locally Lipschitz continuous and twice differentiable almost everywhere (a.e.), which allows us to define its first-order and second-order directional derivatives along the system dynamics. Specifically, the directional derivative of B along the vector field $\boldsymbol{f}(\boldsymbol{x})+\boldsymbol{g}(\boldsymbol{x})\boldsymbol{u}$ is given by

$$\dot{B}(\boldsymbol{x},\boldsymbol{u}) := \nabla B(\boldsymbol{x})^{\mathrm{T}}(\boldsymbol{f}(\boldsymbol{x})+\boldsymbol{g}(\boldsymbol{x})\boldsymbol{u}) \tag{3}$$

and its second-order directional variation is

$$\Phi(\boldsymbol{x},\boldsymbol{u}) := \nabla(\dot{B}(\boldsymbol{x},\boldsymbol{u}))^{\mathrm{T}}(\boldsymbol{f}(\boldsymbol{x})+\boldsymbol{g}(\boldsymbol{x})\boldsymbol{u}) \tag{4}$$

Under ZOH, where $\boldsymbol{u}$ is held constant over each sampling interval, $\Phi(\boldsymbol{x},\boldsymbol{u})$ characterizes the within-interval second-order growth of B along the induced vector field.

To bound the worst-case second-order remainder of B between sampling instants, define

$$\varphi(T,\boldsymbol{x}) = \frac{1}{2}\sup_{z\in\mathcal{R}(\boldsymbol{x},T)\setminus\mathcal{Z},\ \boldsymbol{u}\in\mathcal{U}} |\Phi(\boldsymbol{x},\boldsymbol{u})| \tag{5}$$

where $\mathcal{R}(\boldsymbol{x},T)$ is the set of states reachable from $\boldsymbol{x}$ in one sampling period T under all admissible constant inputs, and $\mathcal{Z}$ is a Lebesgue measure-zero set containing the points where B fails to be twice differentiable. Then $\varphi(T,\boldsymbol{x})$ provides a uniform bound for the second-order term so that the remainder scales as $T^2\varphi(T,\boldsymbol{x})$ in Taylor-type estimates.

Based on these definitions, the following theorem provides a sufficient condition on the one-step change $B(\boldsymbol{x}_{k+1})-B(\boldsymbol{x}_k)$ that ensures the forward invariance of $\mathcal{D}$ under the sampled-data control law $\boldsymbol{u}_k$.

Theorem 1 [20] Consider Eq. (1) implemented with ZOH of sampling period $T>0$. Let $\mathcal{D}\subset\mathbb{R}^n$ be the 0-superlevel set of a continuously differentiable function $B:\mathbb{R}^n\to\mathbb{R}$. If for any pointwise control law $\boldsymbol{u}_k\in\mathcal{U}$ satisfies, for all $k\in\mathbb{Z}_{\geqslant 0}$, we have

$$B(\boldsymbol{x}_{k+1})-B(\boldsymbol{x}_k)\geqslant \psi(T,\boldsymbol{x}_k) \tag{6}$$

$$\psi(T,\boldsymbol{x}_k) = -\gamma T B(\boldsymbol{x}_k) - T^2\varphi(T,\boldsymbol{x}_k) \tag{7}$$

where $\gamma\in(0,1]$ is a design parameter. Then, $\mathcal{D}$ is rendered forward invariant along the closed-loop trajectories of Eq. (1).

Formula (6) is referred to as a DCBF constraint [21]. Given γ, define the admissible input set

$$\mathcal{U}_{\mathrm{dcbf}}(\boldsymbol{x}_k) = \{\boldsymbol{u}_k\in\mathcal{U}: B(\boldsymbol{x}_{k+1})-B(\boldsymbol{x}_k)\geqslant\psi(T,\boldsymbol{x}_k)\}.$$

If $\boldsymbol{x}_0\in\mathcal{D}$ and $\boldsymbol{u}_k\in\mathcal{U}_{\mathrm{dcbf}}(\boldsymbol{x}_k)$ for all k, then $\boldsymbol{x}_k\in\mathcal{D}$ for all $k\in\mathbb{Z}_{\geqslant 0}$. In the sequel, we will enforce Formula (6) to guarantee that the closed-loop trajectories of Eq. (1) remain in $\mathcal{D}$.

Definition 1 Discrete control Lyapunov function [22] Consider Eq. (1) under ZOH with a fixed sampling period $T>0$. A function $V:\mathbb{R}^n\to\mathbb{R}$ is called a discrete control Lyapunov function if there exist constants α_1, α_2, $\alpha_3>0$ such that, for all $x_k\in\mathbb{R}^n$ and $k\in\mathbb{Z}_+$, the following inequalities hold

$$c_1\|\boldsymbol{x}_k\|^2\leqslant V(\boldsymbol{x}_k)\leqslant c_2\|\boldsymbol{x}_k\|^2 \tag{8}$$

$$\Delta V(\boldsymbol{x}_k,\boldsymbol{u}_k)+c_3\|\boldsymbol{x}_k\|^2 \leqslant 0 \tag{9}$$

where $\Delta V(\boldsymbol{x}_k,\boldsymbol{u}_k)=V(\boldsymbol{x}_{k+1})-V(\boldsymbol{x}_k)$.

B. Problem Formulation

Consider N robots indexed by $i \in \mathcal{N} := \{1,2,\ldots,N\}$, which in this paper are taken to be WMRs. The kinematic model of the i-th WMR is given by [23]

$$\begin{cases}\dot{x}_i(t)=v_i(t)\cos\theta_i(t),\\ \dot{y}_i(t)=v_i(t)\sin\theta_i(t),\\ \dot{\theta}_i(t)=\omega_i(t)\end{cases} \tag{10}$$

where $\boldsymbol{p}_i(t)=[\,x_i(t),y_i(t)\,]^{\mathrm{T}} \in \mathbb{R}^2$ denotes the position, $\theta_i(t)\in(-\pi,\pi]$ is the heading angle, and $\boldsymbol{u}_i(t)=[\,v_i(t),\omega_i(t)\,]^{\mathrm{T}}$ is the control input comprising linear and angular velocities. The inputs satisfy $|v_i(t)|\leqslant v_{\max}$ and $|\omega_i(t)|\leqslant\omega_{\max}$. A ZOH with fixed sampling period $T>0$ is adopted. Inputs are updated at sampling instants $t_k=kT$, $k\in\mathbb{Z}_{\geqslant 0}$, and held constant over each interval $[t_k,t_{k+1})$, i.e., $\boldsymbol{u}_i(t)=\boldsymbol{u}_{i,k}$ with $\boldsymbol{u}_{i,k}=[\,v_{i,k},\omega_{i,k}\,]^{\mathrm{T}}$ for $t\in[t_k,t_{k+1})$. We define the sampled state as $\boldsymbol{x}_{i,k}:=[\,\boldsymbol{p}_i(t_k)^{\mathrm{T}},\ \theta_i(t_k)\,]^{\mathrm{T}}=[\,\boldsymbol{p}_{i,k}^{\mathrm{T}},\ \theta_{i,k}\,]^{\mathrm{T}}$.

Given the sampled-data model above, our objective is to design a control strategy that steers the multi-WMR systems from the initial positions $\{\boldsymbol{p}_{i,0}\}_{i=1}^N$ to the desired target positions $\{\boldsymbol{p}_{i,d}\}_{i=1}^N$. Without loss of generality, we assume that the target indexing is pre-assigned so that WMR i is associated with $\boldsymbol{p}_{i,d}$. At each sampling time t_k, define the position-tracking error $\boldsymbol{p}_{i,k}^e:=\boldsymbol{p}_{i,k}-\boldsymbol{p}_{i,d}$. We require finite-time convergence: there exist a settling index $K(\boldsymbol{x}_0)<\infty$ and a tolerance $\varepsilon_p>0$ such that

$$\|\boldsymbol{p}_{i,k}^e\|\leqslant\varepsilon_p,\ \forall i\in\mathcal{N},\ \forall k\geqslant K(\boldsymbol{x}_0).$$

Safety must be ensured throughout the motion to avoid collisions among WMRs. Let $d_s>0$ denotes a prescribed safety margin. The sampled-time safety constraints are

$$\|\boldsymbol{p}_{i,k}-\boldsymbol{p}_{j,k}\| \geqslant d_s+r_i+r_j,\ \forall i,j\in\mathcal{N},\ i\neq j,$$

for all $k\in\mathbb{Z}_{\geqslant 0}$. Between sampling instants, continuous-time safety will be guaranteed by the sampled-data barrier construction introduced later.

In summary, the problem studied in this paper can be formulated as follows: given the initial states $\{\boldsymbol{x}_{i,0}\}_{i=1}^N$ and the desired target positions $\{\boldsymbol{p}_{i,d}\}_{i=1}^N$, design a ZOH control law such that:

(1) Each WMR reaches its assigned target position $\boldsymbol{p}_{i,d}$ within a finite time;

(2) The system trajectories always satisfy the nonholonomic dynamics and input bounds;

(3) Collisions among WMRs are strictly avoided at all time.

III. QP-Based Safe Cooperative Controller

In this section, we introduce the FT-DCLF and derive conditions for finite-time stabilization of sampled-data systems under input constraints. Furthermore, by incorporating both FT-DCLF and DCBF constraints into a QCQP framework, we develop a safety-critical cooperative controller that enables the WMR system to accomplish cooperative tasks within a finite time while ensuring safety.

A. Finite-Time Discrete Control Lyapunov Function

Conventional DCLF constraints guarantee asymptotic stability by ensuring a monotonic decrease of a Lyapunov function. However, in safety-critical and time-sensitive tasks, asymptotic convergence is insufficient, as the system must converge within finite time. Motivated by Ref. [24], we introduce an FT-DCLF to characterize trajectories that reach the equilibrium within a finite number of steps.

Definition 2 Finite-time discrete control Lyapunov function Consider Eq. (1) under ZOH with a fixed sampling period $T>0$. A map $V:\mathbb{R}^n\to\mathbb{R}$ is called a finite-time discrete control Lyapunov function with a settling time $K(\boldsymbol{x}_0)>0$ if there exist a control input $\boldsymbol{u}_k\in\mathcal{U}$ and constants c_1, c_2, $c_3>0$, $\alpha\in(0,1)$ such that, for all $\boldsymbol{x}_k\in\mathbb{R}^n$ and $k\in\mathbb{Z}_{\geqslant 0}$, the following inequalities hold

$$c_1\|\boldsymbol{x}_k\|^2\leqslant V(\boldsymbol{x}_k)\leqslant c_2\|\boldsymbol{x}_k\|^2 \tag{11}$$

$$\Delta V(\boldsymbol{x}_k,\boldsymbol{u}_k)+Q(\boldsymbol{x}_k)\leqslant 0 \tag{12}$$

where $\Delta V(\boldsymbol{x}_k,\boldsymbol{u}_k)=V(\boldsymbol{x}_{k+1})-V(\boldsymbol{x}_k)$ and $Q(\boldsymbol{x}_k)=\min\{V(\boldsymbol{x}_k),\ c_3V(\boldsymbol{x}_k)^{\alpha}\}$.

The existence of an FT-DCLF implies that a family of controllers can be designed to drive the closed-loop trajectory of Eq. (10) to the equilibrium point within a setting time $K(\boldsymbol{x}_0)$. In particular, given an FT-DCLF $V(\cdot)$, the admissible control set that satisfies condition in Formula (12) can be defined as

$$\mathcal{K}_{\mathrm{dclf}}(\boldsymbol{x}_k)=\{\boldsymbol{u}_k\in\mathcal{U}:\Delta V(\boldsymbol{x}_k,\boldsymbol{u}_k)+Q(\boldsymbol{x}_k)\leqslant 0\} \tag{13}$$

By selecting control inputs from the set $\mathcal{K}_{\mathrm{dclf}}$, the finite-time convergence of Eq. (10) can be guaranteed through a following direct application of Theorem 2.

Theorem 2 Consider Eq. (10) under ZOH with a fixed sampling period $T>0$. Assume the existence of a continuous function $V(\cdot):\mathbb{R}^n\to\mathbb{R}$ that is an FT-DCLF. If any pointwise control law $\boldsymbol{k}_b:\mathbb{R}^n\to\mathbb{R}^m$ satisfies $\boldsymbol{k}_b(\boldsymbol{x})\in\mathcal{K}_{\mathrm{dclf}}$ for all $\boldsymbol{x}\in\mathbb{R}^n$, then the origin of the error dynamics is finite-time stable. Moreover, there exists a settling-time function $K(\boldsymbol{x}_0):\mathbb{R}^n\to\mathbb{Z}_{\geqslant 0}$ such that either

$$K(\boldsymbol{x}_0)\leqslant\begin{cases}1,\ V(\boldsymbol{x}_0)\leqslant r_\star;\\ \left\lceil\dfrac{\ln\left(\frac{V(\boldsymbol{x}_0)}{r_\star}\right)}{-\ln(1-c_3V(\boldsymbol{x}_0)^{\alpha-1})}\right\rceil+1,\ V(\boldsymbol{x}_0)>r_\star\end{cases} \tag{14}$$

where $r_\star:=c_3^{\frac{1}{1-\alpha}}$ defined as the capture radius.

Proof Consider the scalar sequence

$$z_{k+1}=z_k-w(z_k),\ z_0:=V(\boldsymbol{x}_0) \tag{15}$$

where $w(s):=\min\{c\cdot s^{\alpha},\ s\}$, $c>0$, $\alpha\in(0,1)$. Since V is positive definite and nonnegative, we have $z_0=V(\boldsymbol{x}_0)\geqslant 0$. For any $s\geqslant 0$, $w(s)\in[0,s]$, therefore

$$0\leqslant z_{k+1}=z_k-w(z_k)\leqslant z_k,\ \forall k\in\mathbb{Z}_{\geqslant 0}.$$

Hence, the sequence $\{z_k\}$ is nonnegative and nonincreasing.

According to the comparison lemma [25], it holds that

$$0 \leqslant V(\boldsymbol{x}_k) \leqslant z_k, \forall k \in \mathbb{Z}_{\geqslant 0} \tag{16}$$

Note that if $z_k \leqslant r_\star$, then $c_3 z_k^\alpha \geqslant z_k$ so that $\psi(z_k) = z_k$ and hence $z_{k+1} = 0$. If $z_k > r_\star$, then $w(z_k) = c_3 z_k^\alpha \in (0, z_k)$ and

$$\frac{z_{k+1}}{z_k} = 1 - \xi_k,\ \xi_k := c_3\, z_k^{\alpha-1} \in (0,1).$$

Because $\alpha - 1 < 0$ and $\{z_k\}$ is nonincreasing, $\{\xi_k\}$ is nondecreasing and thus

$$z_k = z_0 \prod_{\varrho=0}^{k-1} (1-\xi_\varrho) \leqslant z_0 (1-\xi_0)^k \tag{17}$$

where $\xi_0 := c_3\, z_0^{\alpha-1} = c_3 V(\boldsymbol{x}_0)^{\alpha-1}$.

A sufficient condition to enter the capture set $[0, r_\star]$ is $z_k \leqslant r_\star$. From Formula (17) this is guaranteed if $z_0(1-\xi_0)^k \leqslant r_\star$, and we have

$$k \geqslant \frac{\ln\left(\frac{z_0}{r_\star}\right)}{-\ln(1-\xi_0)} = \frac{\ln\left(\frac{V(\boldsymbol{x}_0)}{r_\star}\right)}{-\ln(1-c_3 V(\boldsymbol{x}_0)^{\alpha-1})} \tag{18}$$

Let

$$K_{\text{enter}}\ (\boldsymbol{x}_0) := \left\lceil \frac{\ln\left(\frac{V(\boldsymbol{x}_0)}{r_\star}\right)}{-\ln(1-c_3 V(\boldsymbol{x}_0)^{\alpha-1})} \right\rceil \tag{19}$$

Then $k \geqslant K_{\text{enter}}(\boldsymbol{x}_0)$ implies $z_k \leqslant r_\star$, and by Formula (16) also

$$V(\boldsymbol{x}_k) \leqslant z_k \leqslant r_\star \tag{20}$$

At such k, we have $c_3 V(\boldsymbol{x}_k)^\alpha \geqslant V(\boldsymbol{x}_k)$, whence $w(V(\boldsymbol{x}_k)) = V(\boldsymbol{x}_k)$ and

$$0 \leqslant V(\boldsymbol{x}_{k+1}) \leqslant V(\boldsymbol{x}_k) - w(V(\boldsymbol{x}_k)) = 0,$$

so $V(\boldsymbol{x}_{k+1}) = 0$. Since V is positive definite ($V(\boldsymbol{x}) = 0 \Leftrightarrow \boldsymbol{x} = 0$), it follows that $\boldsymbol{x}_{k+1} = 0$. Substituting $\boldsymbol{x}_{k+1} = 0$ into Formula (12) shows $V(\boldsymbol{x}_{k+2}) \leqslant 0$, hence $V(\boldsymbol{x}_{k+2}) = 0$ and $\boldsymbol{x}_{k+2} = 0$; thus the origin is forward invariant once reached. Combining with Formula (20) gives the settling-time bound in Eq. (19). Therefore, the origin is finite-time stable.

In summary, the origin is reached in at most the number of steps given by

$$K(x_0) = \begin{cases} 1,\ V(x_0) \leqslant r_\star; \\ K_{\text{enter}}(x_0) + 1,\ V(x_0) > r_\star \end{cases} \tag{21}$$

where $K_{\text{enter}}(\cdot)$ is given in Eq. (19). This completes the proof. ■

Thus, under sampled-data implementation, the FT-DCLF guarantees convergence of Eq. (10) to the goal position. Since FT-DCLF alone does not encode safety, we next synthesize a QP that unifies FT-DCLF with DCBF constraints.

B. QP-Based Formation Controller Design

We design a safety-critical collaborative controller by integrating FT-DCLF and DCBF constraints within a QP. The FT-DCLF enforces finite-time convergence to the desired configuration, while the DCBF guarantees collision avoidance throughout the maneuver.

a. Safety Control

To avoid inter-WMR collisions, define

$$B_{ij}^r(\boldsymbol{x}_i, \boldsymbol{x}_j) := \|\boldsymbol{p}_i - \boldsymbol{p}_j\|^2 - \rho_r^2 \tag{22}$$

where $\rho_r := d_s + r_i + r_j$ with $r_j > 0$ is the radius of WMR j.

For the DCBF in Eq. (22), a first-order propagation of the point yields

$$\boldsymbol{p}_i^{k+1} - \boldsymbol{p}_i^k = \Delta t\, \boldsymbol{a}_i^k \tag{23}$$

where $\boldsymbol{a}_i^k = \boldsymbol{J}_i^k \boldsymbol{u}_i^k$, $\boldsymbol{J}_i^k := \begin{bmatrix} \cos\theta_i^k & 0 \\ \sin\theta_i^k & 0 \end{bmatrix}$. So, we have

$$\Delta B_{ij}^r = 2\Delta t (\boldsymbol{p}_i^k - \boldsymbol{p}_j^k)^{\mathrm{T}} \boldsymbol{b}_i^k + \Delta t^2 \|\boldsymbol{b}_i^k\|_2^2 \tag{24}$$

where $\boldsymbol{b}_i^k = \boldsymbol{J}_i^k \boldsymbol{u}_i^k - \boldsymbol{J}_j^k \boldsymbol{u}_j^k$.

Applying Formula (6) to Eq. (24) yields, at time k

$$\Delta B_{ij}^r \geqslant -\gamma \Delta t B_{ij}^r(k) - \Delta t^2 \varphi_{ij}^k + \delta_{r,ij},\ \forall j \neq i \in \mathcal{N} \tag{25}$$

with design parameters $\gamma \in (0,1]$ and slack variables $\delta_{r,ij} \geqslant 0$. The terms $\varphi_{ij}^k := \varphi(\Delta t, \boldsymbol{x}_i^k, \boldsymbol{x}_j^k)$ denote computable upper bounds on the higher-order terms, which can be obtained from known input bounds together with an over-approximation of the reachable set.

At each sampling instant t_k, we enforce the DCBF condition in Formula (6) with $B = B_{ij}^r$ constructed from Eq. (22) to maintain forward invariance of the safe sets $\{B \geqslant 0\}$. These DCBF constraints ensure that each WMR preserves a prescribed minimum clearance from neighboring WMRs, thereby guaranteeing safety throughout the process.

b. Performance Control

In addition to safety, the controller must drive each WMR i to its target within a finite number of sampling steps. Consistent with the DCBF design, we define the position error

$$\tilde{\boldsymbol{p}}_i^k := \boldsymbol{p}_i^k - \boldsymbol{p}_{i,d},$$

where $\boldsymbol{p}_{i,d} \in \mathbb{R}^2$ is the assigned target of WMR i. Choose the FT-DCLF

$$V_i(\tilde{\boldsymbol{p}}_i^k) := \frac{1}{2} \|\tilde{\boldsymbol{p}}_i^k\|_2^2 \tag{26}$$

A first-order propagation of the point yields

$$V_i(\tilde{\boldsymbol{p}}_i^{k+1}) - V_i(\tilde{\boldsymbol{p}}_i^k) = \boldsymbol{c}_i^{k\mathrm{T}} \boldsymbol{u}_i^k + \frac{\Delta t^2}{2} \|\boldsymbol{J}_i^k \boldsymbol{u}_i^k\|_2^2 \tag{27}$$

where $\boldsymbol{c}_i^k := \Delta t (\tilde{\boldsymbol{p}}_i^k)^{\mathrm{T}} \boldsymbol{J}_i^k$. A sufficient FT-DCLF constraint is therefore

$$\boldsymbol{c}_i^{k\mathrm{T}} \boldsymbol{u}_i^k + \frac{\Delta t^2}{2} \|\boldsymbol{J}_i^k \boldsymbol{u}_i^k\|_2^2 \leqslant -Q_i(\tilde{\boldsymbol{p}}_i^k) + \delta_i \tag{28}$$

For the heading, define the reference angle $\theta_{\text{ref},i}^k$ as the bearing-to-goal $\operatorname{atan2}(y_{i,d} - y_i^k,\ x_{i,d} - x_i^k)$, and let the wrapped heading error be

$$e_{\theta,i}^k := \operatorname{wrap}(\theta_i^k - \theta_{\text{ref},i}^k),\ \operatorname{wrap}(\cdot) \in (-\pi, \pi].$$

Choose the FT-DCLF as

$$V_{\theta,i}(e_{\theta,i}^k) := 1 - \cos(e_{\theta,i}^k) \tag{29}$$

A first-order propagation of the point yields

$$V_{0.i}(e_{\theta,i}^{k+1}) - V_{0,i}(e_{\theta,i}^k) = \boldsymbol{d}_i^{k\mathrm{T}} \boldsymbol{u}_i^k + \frac{\Delta t^2}{2} \|\boldsymbol{H}_i^k \boldsymbol{u}_i^k\|_2^2 \tag{30}$$

where

$$\boldsymbol{d}_i^k := \Delta t \sin(e_{\theta,i}^k) \cdot [0 \;\; 1], \;\; \boldsymbol{H}_i^k := \sqrt{\cos(e_{\theta,i}^k)} \cdot [0 \;\; 1].$$

A sufficient FT-DCLF constraint is therefore

$$\boldsymbol{d}_i^{k\mathrm{T}} \boldsymbol{u}_i^k + \frac{\Delta t^2}{2} \|\boldsymbol{H}_i^k \boldsymbol{u}_i^k\|_2^2 \leqslant -Q_{\theta,i}(e_{\theta,i}^k) + \delta_{\theta,i} \tag{31}$$

with $Q_{\theta,i}(e_{\theta,i}^k) > 0$ and slack variable $\delta_{\theta,i} \geqslant 0$.

The resulting constraint in Formulas (28) and (31) is a convex quadratic function of the control inputs (v_i^k, ω_i^k). Hence, it can be formulated as a quadratic constrained quadratic program and solved jointly with the DCBF constraints within a unified optimization framework.

c. Controller Design for WMR Navigation

To jointly enforce safety and finite-time convergence, we embed the DCBF constraints in Formula (25) and the FT-DCLF constraint in Formulas (28) and (31) into a single convex program that is solved at each sampling instant.

Define the obstacle and WMR neighbor sets of WMR i at step k as

$$\mathcal{N}_i^k := \{ j \in \mathcal{N} \setminus \{i\} \mid B_{ij}^r(k) \leqslant \varepsilon_r \} \tag{32}$$

with small activation margins $\varepsilon_r > 0$. Let $z_i = \{\boldsymbol{u}_i^k, \delta_{p,i}, \delta_{\theta,i}, \{\delta_{r,ij}\}_{j \in \mathcal{N}_i}\}$, then consider the QCQP

$$z_i^\star = \arg\min_{z_i} \frac{1}{2} (\boldsymbol{u}_i^k)^\mathrm{T} R_i \boldsymbol{u}_i^k + w_p \delta_{p,i} + w_\theta \delta_{\theta,i} + \sum_{i \neq j \in N_i^k} w_{r,ij} \delta_{r,ij} \tag{33a}$$

$$\text{s.t.,} \;\; \boldsymbol{a}_i^{k\mathrm{T}} \boldsymbol{u}_i^k + \frac{\Delta t^2}{2} \|\boldsymbol{J}_i^k \boldsymbol{u}_i^k\|_2^2 \leqslant -Q_i(\tilde{\boldsymbol{p}}_i^k) + \delta_{p,i} \tag{33b}$$

$$\boldsymbol{d}_i^{k\mathrm{T}} \boldsymbol{u}_i^k + \frac{\Delta t^2}{2} \|\boldsymbol{H}_i^k \boldsymbol{u}_i^k\|_2^2 \leqslant -Q_{\theta,i}(e_{\theta,i}^k) + \delta_{\theta,i} \tag{33c}$$

$$\Delta B_{ij}^r \geqslant -\gamma \Delta t B_{ij}^r(k) - \Delta t^2 \varphi_{ij}^k + \delta_{r,ij} \tag{33d}$$

$$v_{\min} \leqslant v_i^k \leqslant v_{\max}, \quad \omega_{\min} \leqslant \omega_i^k \leqslant \omega_{\max} \tag{33e}$$

$$\delta_{p,i} \geqslant 0, \quad \delta_{\theta,i} \geqslant 0, \quad \delta_{r,ij} \geqslant 0 \tag{33f}$$

Here $R_i \succ 0$ and $w_p, w_\theta, w_{r,ij} > 0$ penalize control effort and slack usage. $Q_i(\cdot) = -\min\{V(\cdot), c_3 V(\cdot)^\alpha\}$ with $c_3 > 0$, $\alpha \in (0,1)$.

Remark 1 Larger γ enlarges the right-hand side of Formula (33d), yielding more conservative safety margins (farther from the boundary) but potentially shrinking feasibility under tight input bounds. Smaller values relax the safety decay rate and improve feasibility at the expense of reduced separation; the slacks $\delta_{r,ij}$ provide a soft guarantee and should be penalized heavily in Eq. (33a).

IV. SIMULATION

In this section, we evaluate the proposed safety-critical coordination controller for multi-WMR navigation under nonholonomic kinematics and strict collision avoidance. We consider a representative scenario: position swapping. The proposed method is compared with the conventional exponential DCLF-DCBF (EXP-DCLF-DCBF) [22]. The continuous-time dynamics are discretized using the forward Euler method with sampling period Δt. All simulations are conducted in MATLAB, the models are constructed in CasADi, and the resulting convex programs are solved using IPOPT on a desktop computer (Intel i7-4970, 3.6 GHz).

A. Simulation Setup

Seven WMRs are assigned target positions located in distinct sectors of the workspace, yielding a cyclic position-swapping task. This evaluation constitutes a standardized test conducted under identical initial conditions and safety constraints, enabling a fair comparison between the proposed FT-DCLF controller and the baseline EXP-DCLF approach.

Inter-WMR safety is enforced via DCBF constraints. At each sampling step k, only neighbors within the activation sets are considered, namely the WMR set $\mathcal{N}_i^k$. The proposed controller solves the distributed optimization program in Formula (33). The baseline method differs only in the performance certificate, replacing the FT-DCLF constraint with exponential DCLFs for position and heading. All remaining constraints and weights are kept identical across both methods.

The main parameter settings are summarized: sampling period $\Delta t = 0.08$ s, safety buffer $d_s = 0.15$ m, WMR radius $r_i = r_j = 0.15$ m, $c_3 = 0.5$, $\alpha = 0.6$, speed bounds $[v_{\min}, v_{\max}] = [0, 5]$ m/s, turn-rate bounds $[\omega_{\min}, \omega_{\max}] = [-1, 1]$ rad/s, DCBF gains $\gamma = 0.6$, slack weights $(w_p, w_\theta, w_{r,ij}) = (10^3, 10^4, 10^4)$, control weight $R_i = \mathrm{diag}(1, 0.5)$, and neighbor activation thresholds $\varepsilon_r = 1.5$ m. The initial positions are defined as $\boldsymbol{p}_{i,0} \in \{(-5, -0.4), (5, 0.4), (-0.4, 5), (0.4, -5), (3.2, 3.8), (-3.2, -3.8), (-3.8, 3.2), (3.8, -3.2)\}$. The desired target positions are defined as $\boldsymbol{p}_{i,d} \in \{(4.5, 0), (-4.5, 0), (0, -4.5), (0, 4.2), (-3.5, -3.4), (3.4, 3.5), (3.5, -3.4), (-3.4, 3.5)\}$.

B. Simulation Results

Figs. 1 and 2 illustrate that both the EXP-DCLF method and the FT-DCLF method can successfully accomplish the position-swapping task. For a more detailed visualization of the multi-WMR systems's motion, please refer to the attached

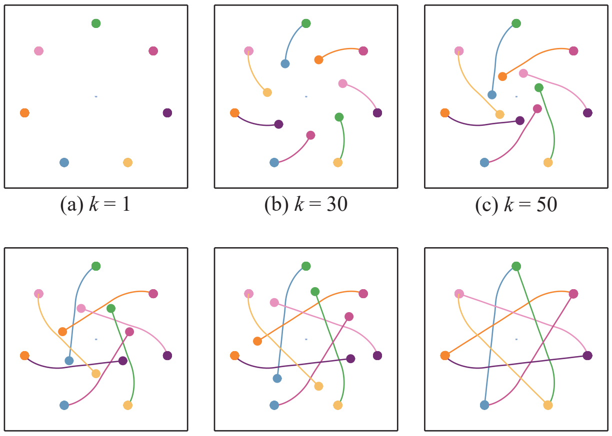

(a) $k = 1$ (b) $k = 30$ (c) $k = 50$ (d) $k = 75$ (e) $k = 100$ (f) $k = 170$

Fig. 1 Position-swapping trajectories with EXP-DCLF-DCBF.

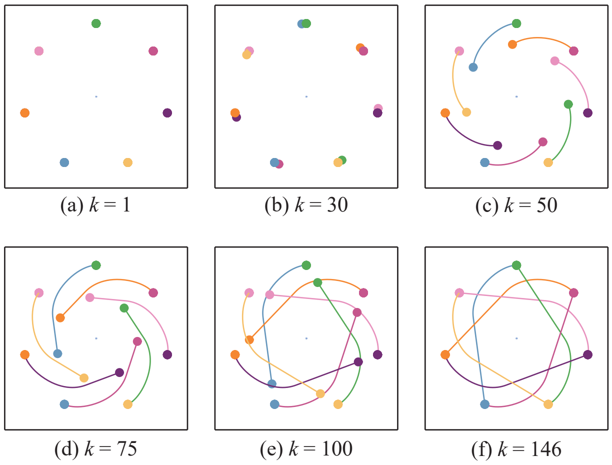

Fig. 2 Position-swapping trajectories with the proposed method.

video (https://youtube.com/shorts/yfpU-uwfdm8?feature=share).

Based on the control input analysis in Fig. 3, it is evident that the angular velocity ω curve of the EXP-DCLF method exhibits substantial fluctuations, especially in the early stages, with a larger magnitude of change. This indicates that the control input in the early phase is unstable, requiring further adjustments to achieve a stable state. Such fluctuations not only consume more energy but may also lead to system instability. In contrast, the FT-DCLF exhibits smoother control input ω changes throughout the process, particularly in the later stages, where the angular velocity curve stabilizes, indicating that this method offers a more gradual adjustment of control inputs, leading to more efficient control.

Fig. 4 illustrates the variation of the average real-time distance to the target over time for both methods. The EXP-DCLF method shows a rapid initial convergence of the average real-time distance, but its convergence rate slows down over time. In comparison, when using the FT-DCLF method, the WMR's average real-time distance converges more quickly and ultimately reaches a lower error value. This indicates that the FT-DCLF method performs better in terms of both convergence speed and stability.

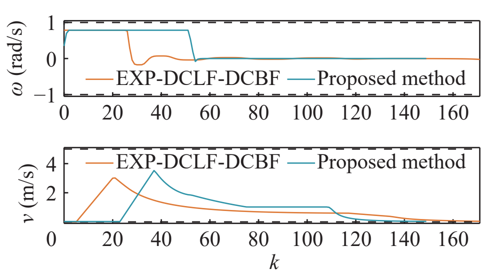

Fig. 3 Average control inputs for multi-WMRs.

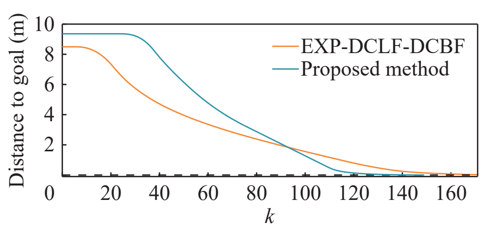

Fig. 4 Average real-time distance to goal for multi-WMRs.

V. CONCLUSIONS

In this paper, we addressed the safety-critical problem of multi-robot coordination under sampled-data control by introducing a unified framework that integrates an incremental DCBF and an FT-DCLF within a single QCQP with feasibility-aiding slack and input bounds. We established all-time safety by enforcing gap-compensated DCBF constraints, and we derived sufficient conditions to ensure finite-time convergence within a preset number of sampling steps. Simulation studies on multi-WMR systems demonstrated faster convergence and stronger safety guarantees compared with conventional DCLF-DCBF baselines. Future work will extend the framework to systems with disturbances and model uncertainty to facilitate deployment in practical platforms.

ACKNOWLEDGMENT

This work was supported by the Joint Fund of the National Natural Science Foundation of China (No. U24A20263) and the National Natural Science Foundation of China (No. 62473071).

REFERENCES

[1] H. Liu, Y. P. Tsang, C. K. M. Lee, and C. H. Wu, UAV trajectory planning via viewpoint resampling for autonomous remote inspection of industrial facilities, *IEEE Trans. Industr. Inform.*, 2024, 20(5), 7492–7501.

[2] B. Li and H. Ma, Double-deck multi-agent pickup and delivery: Multi-robot rearrangement in large-scale warehouses, *IEEE Robot. Autom. Lett.*, 2023, 8(6), 3701–3708.

[3] X. Cao, M. Li, Y. Tao, and P. Lu, HMA-SAR: Multi-agent search and rescue for unknown located dynamic targets in completely unknown environments, *IEEE Robot. Autom. Lett.*, 2024, 9(6), 5567–5574.

[4] Y. Liu and N. Zhao, Adaptive dynamic event-triggered asymptotic control for uncertain nonlinear systems, *Chaos Solitons Fractals*, 2024, 189, 115597.

[5] Y. An and Y. Liu, Observer-based dynamic event-triggered adaptive control for uncertain nonlinear strict-feedback systems, *Syst. Control Lett.*, 2024, 183, 105700.

[6] A. D. Ames, X. Xu, J. W. Grizzle, and P. Tabuada, Control barrier function based quadratic programs for safety critical systems, *IEEE Trans. Autom. Control*, 2017, 62(8), 3861–3876.

[7] D. Li, B. Zhang, R. Law, E. Wu, and X. Xu, Error constrained-formation path-following method with disturbance elimination for multisnake robots, *IEEE Trans. Ind. Electron.*, 2024, 71(5), 4987–4998.

[8] W. Han, J. Wang, Y. Wang, and B. Xu, Multi-UAV flocking control with a hierarchical collective behavior pattern inspired by sheep, *IEEE Trans. Aerosp. Electron. Syst.*, 2024, 60(2), 2267–2276.

[9] L. Li, P. Shi, C. K. Ahn, Y. J. Kim, and W. Xing, Tube-based model predictive full containment control for stochastic multiagent systems, *IEEE Trans. Autom. Control*, 2023, 68(7), 4024–4037.

[10] X. Li, Z. Jing, and P. Ju, Leader-follower based online reinforcement learning algorithm in problem with hierarchy decision makers, *Int. J. Intell. Control Syst.*, 2024, 29(1), 48–58.

[11] T. Xu, J. Liu, Z. Zhang, G. Chen, D. Cui, and H. Li, Distributed MPC for trajectory tracking and formation control of multi-UAVs with leader-follower structure, *IEEE Access*, 2023, 11, 128762–128773.

[12] G. Wang, X. Wang, and S. Li, Signal generator based finite-time formation control for disturbed heterogeneous multi-agent systems, *J. Franklin Inst.*, 2022, 359(2), 1041–1061.

[13] F. Wang, S. He, C. Zhou, Y. Gao, and Q. Zong, Distributed practical finite-time formation control of quadrotor UAVs based on finite-time event-triggered disturbance observer, *IEEE Syst. J.*, 2024, 18(1), 355–366.

[14] S. Chang, Y. Wang, Z. Zuo, and H. Yang, Fixed-time formation control

for wheeled mobile robots with prescribed performance, *IEEE Trans. Control Syst. Technol.*, 2022, 30(2), 844–851.

[15] C. Mu and J. Peng, Learning-based cooperative multiagent formation control with collision avoidance, *IEEE Trans. Syst. Man Cybern. Syst.*, 2022, 52(12), 7341–7352.

[16] A. Schwab and J. Lunze, Formation control over Delaunay triangulation networks with guaranteed collision avoidance, *IEEE Trans. Control Netw. Syst.*, 2023, 10(1), 419–429.

[17] J. van den Berg, S. J. Guy, M. Lin, and D. Manocha, Reciprocal *n*-body collision avoidance, in *Robotics Research*. Berlin, Germany: Springer, 2011, 3–19.

[18] Y. Chen, A. Singletary, and A. D. Ames, Guaranteed obstacle avoidance for multi-robot operations with limited actuation: A control barrier function approach, *IEEE Control Syst. Lett.*, 2021, 5(1), 127–132.

[19] L. Wang, A. D. Ames, and M. Egerstedt, Safety barrier certificates for collisions-free multirobot systems, *IEEE Trans. Robot.*, 2017, 33(3), 661–674.

[20] J. Breeden, K. Garg, and D. Panagou, Control barrier functions in sampled-data systems, *IEEE Control Syst. Lett.*, 2022, 6, 367–372.

[21] J. Zeng, B. Zhang, and K. Sreenath, Safety-critical model predictive control with discrete-time control barrier function, in *Proc. American Control Conference*, New Orleans, LA, USA, 2021, 3882–3889.

[22] A. Agrawal and K. Sreenath, Discrete control barrier functions for safety-critical control of discrete systems with application to bipedal robot navigation, in *Proc. Robotics: Science and Systems*, Cambridge, MA, USA, 2017.

[23] P. Anand, A. P. Aguiar, and P. B. Sujit, Circumnavigation of UAVs integrating QP-based CLF and CBF in a cooperative path-following framework, in *Proc. 63rd IEEE Conference on Decision and Control*, Milan, Italy, 2024, 6206–6211.

[24] W. M. Haddad and J. Lee, Finite-time stability of discrete autonomous systems, *Automatica*, 2020, 122, 109282.

[25] Z.-P. Jiang and Y. Wang, A converse Lyapunov theorem for discrete-time systems with disturbances, *Syst. Control Lett.*, 2002, 45(1), 49–58.

Liang Gao received the MS degree from School of Harbin Normal University, Harbin, China, in 2020. He is currently pursuing the PhD degree in control science and engineering at Dalian University of Technology, Dalian, China. His research interests include multi-robot systems, model predictive control, and nonlinear control systems.

Yongfeng Gao received the BS and PhD degrees from Dalian University of Technology, Dalian, China, in 2009 and 2017, respectively. He is currently an associate professor at Dalian University of Technology, Dalian, China. His research interests include adaptive control, model predictive control, and nonlinear control systems.

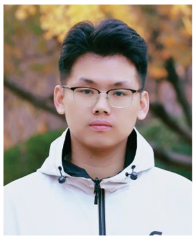

Mingde He received the BS degree from Taiyuan University of Technology, Shanxi, China, in 2022. He is currently pursuing the MS degree in control engineering at Dalian University of Technology, Dalian, China. His research interests include multi-agent systems, model predictive control, and nonlinear systems.

Changyi Xu received the MS degree in condensed matter physics from University of Chinese Academy of Sciences, Beijing, China, in 2016, and the PhD degree in automation from École Nationale Supérieure de Lyon, Lyon, France, in 2020. He is currently an associate professor at Dalian University of Technology, Dalian, China. His research interests include digital twins, robotics, artificial intelligence, aeroengines, discrete event systems, electronic information science, control theory, and reliability.

Yuhu Wu received the PhD degree in mathematics from Harbin Institute of Technology, Harbin, China, in 2012. Since 2012, he has held an assistant professor position at Harbin University of Science and Technology, Harbin, China. He was a postdoctoral researcher at Sophia University, Tokyo, Japan, from 2012 to 2015. In 2015, he joined School of Control Science and Engineering, Dalian University of Technology, Dalian, China, where he is currently a full professor. His research interests include optimization, game-based control, and nonlinear control theory with applications to Boolean networks, automotive powertrain systems, and unmanned aerial vehicles.